

Neutron hole states of $^{93,95}\text{Mo}^\dagger$

P. K. Bindal, D. H. Youngblood, and R. L. Kozub*

Cyclotron Institute and Physics Department, Texas A&M University, College Station, Texas 77843

(Received 4 October 1976)

The (p,d) and (d,t) reactions on ^{94}Mo and ^{96}Mo have been used at bombarding energies of ~ 40 MeV to populate neutron hole states of ^{93}Mo and ^{95}Mo . Excitation energies and angular distributions were measured for levels up to ~ 5 MeV in excitation. A distorted-wave Born approximation analysis was used to make l assignments and to obtain spectroscopic factors. Three distinct groups of weakly excited levels, one corresponding to $l = 4$ and two corresponding to $l = 1$, were observed above 2.3 MeV excitation in both nuclei. A quasiparticle-core coupling model is used to predict the properties of $^{93,95}\text{Mo}$ nuclei and fair agreement with the experiments is obtained.

NUCLEAR REACTIONS, NUCLEAR STRUCTURE $^{94,96}\text{Mo}(p,d)$, $^{94,96}\text{Mo}(d,t)$, $E \approx 40$ MeV, measured $\sigma(\theta)$, $^{93,95}\text{Mo}$ levels, deduced l , C^2S_n ; calculated J , π , S_n , quasiparticle-core coupling model.

I. INTRODUCTION

This paper concludes a series of nuclear structure studies of proton particle¹ and hole² states and neutron hole states^{3,4} of odd- A nuclei in the $A = 90-100$ region. The study of proton hole states in $^{95,97,99}\text{Nb}$ populated by the $(d,^3\text{He})$ reaction² revealed that in the $^{96,98,100}\text{Mo}$ ground states, the $2p_{1/2}$ and $2p_{3/2}$ subshells are not completely filled, the $1g_{9/2}$ orbit is about 25% filled, and there is a small occupation of the $2d_{5/2}$ orbital. Moreover, there is little change in the proton configuration as more neutrons are added above the $1g_{9/2}$ neutron orbit. The study of the isobaric analog states³ excited in neutron pickup reactions on the Mo isotopes revealed a pronounced decrease in the hole strength with increasing mass number as well as fluctuations in the ratio of $C^2S_n(p,d)/C^2S_n(d,t)$.

In the studies⁴ of neutron hole states of ^{97}Mo and ^{99}Mo only about half of the $1g_{9/2}$, $2p_{1/2}$, and $2p_{3/2}$ strengths were observed up to 4.5 MeV excitation. The ground states of ^{98}Mo and ^{100}Mo contain significant contributions from the $3s_{1/2}$, $2d_{3/2}$, $2d_{5/2}$, and $1g_{7/2}$ neutron orbits along with a small admixture of the $1h_{11/2}$ shell. Another interesting aspect of this study is that high-lying levels (above 2.7 and 2.1 MeV in ^{97}Mo and ^{99}Mo , respectively) could be divided into three distinct groups of weakly excited levels, one corresponding to mainly $l = 4$ transfer and two corresponding to mainly $l = 1$ transfer. The present work continues the studies of neutron hole states into the lighter Mo isotopes ^{93}Mo and ^{95}Mo , where similar effects are observed.

The information on the level structures of ^{93}Mo and ^{95}Mo has been compiled in the Nuclear Data

Sheets.^{5,6} Spectroscopic information on the neutron hole states has previously been obtained up to 4.8 MeV in ^{93}Mo using the $^{94}\text{Mo}(p,d)^{93}\text{Mo}$ reaction,⁷ and up to ~ 3.5 MeV in ^{95}Mo using the $^{96}\text{Mo}(d,t)^{95}\text{Mo}$ reaction.^{8,9} In the present study, nuclear structure information was obtained for levels up to 5.15 MeV in ^{93}Mo and up to 4.8 MeV in ^{95}Mo using (p,d) and (d,t) reactions on ^{94}Mo and ^{96}Mo targets. The resolution of ~ 50 keV in the present work has enabled us to resolve several groups of levels in ^{93}Mo which were not resolved by Moinster *et al.*,⁷ as their resolution was ~ 100 keV. Finally, the results are compared with the predictions of a quasiparticle-core coupling model which has been applied by us in our previous studies of neutron and proton hole states^{2,4} in this mass region.

II. EXPERIMENTAL PROCEDURE

The details of the experimental setup and data analysis have been described elsewhere.^{1,4} Self-supporting ^{94}Mo and ^{96}Mo foils, enriched to greater than 94% in the desired isotope, were bombarded with 38.6-MeV protons and 40.6-MeV deuterons accelerated by the Texas A & M University cyclotron. The target thicknesses were approximately 1 mg/cm^2 , determined by weighing. Two silicon detector telescopes spaced 5° apart were used simultaneously to reduce data acquisition time and selected data points were checked by measurements with both systems. The telescopes consisted of $700 \mu\text{m}$ ΔE , 3 mm E , and 2 mm veto detectors for the forward stack with 1 mm ΔE , 3 mm E , and 1 mm veto detectors for the other stack for the (p,d) reaction. For the (d,t) studies, 1 mm ΔE , 3 mm E , and $700 \mu\text{m}$ veto detectors were used for the forward stack and $500 \mu\text{m}$ ΔE ,

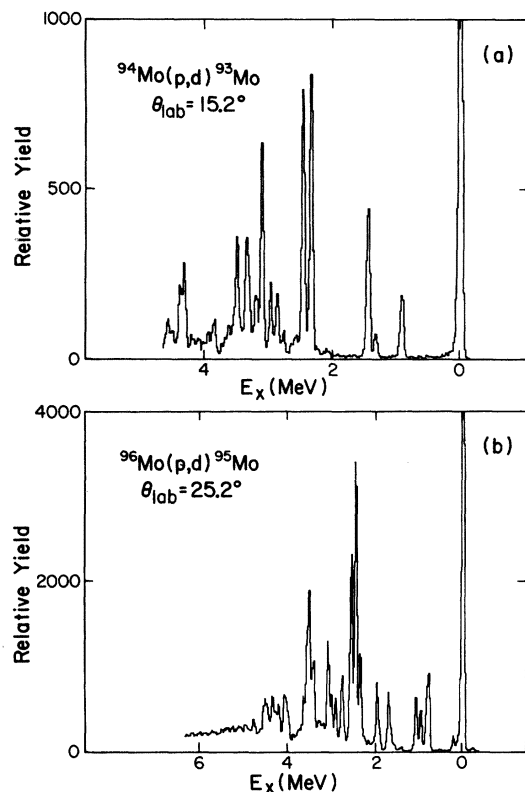


FIG. 1. Spectra of the $^{94}\text{Mo}(p,d)^{93}\text{Mo}$ and $^{96}\text{Mo}(p,d)^{95}\text{Mo}$ reactions.

3 mm E , and 1.5 mm veto detectors for the other stack. The veto detectors served to eliminate pulses due to the elastically scattered particles. The overall resolution obtained was about 50 keV full width at half maximum. Typical deuteron spectra are shown in Fig. 1 for ^{93}Mo and ^{95}Mo . Deuteron and triton spectra actually extend up to about 15 MeV in order to extract information on the isobaric analog states, the subject of previous communications,³ where energy calibration and cross-section normalization techniques are also explained. Due to the high density of levels in the high excitation region, a multipeak fitting program,

described previously,⁴ was used in analyzing the spectra.

III. DISTORTED-WAVE BORN APPROXIMATION AND EXPERIMENTAL RESULTS

Distorted-wave Born approximation (DWBA) calculations including finite-range and nonlocal (FRNL) corrections were performed with the computer code DWUCK¹⁰ using the optical model parameters¹¹⁻¹³ given in Table I. The calculated and experimental cross sections are related by

$$\left(\frac{d\sigma}{d\Omega}\right)_{\text{exp}} = \frac{NC^2S}{2J+1} \left(\frac{d\sigma}{d\Omega}\right)_{\text{DWUCK}}, \quad (1)$$

where J is the transferred angular momentum, N is the normalization constant determined from the internal structure of the projectiles, and C^2S is the spectroscopic factor. We have used a value of $N=2.54$ for the (p,d) reaction and 3.33 for the (d,t) reaction.

A. ^{93}Mo

The information on energy levels, l -value assignments, and spectroscopic factors for ^{93}Mo obtained in the present study is summarized and compared with previous studies in Table II. Our energy locations, J^π assignments, and the spectroscopic factors agree very well with previous studies. The (d,t) and the $(^3\text{He},\alpha)$ reactions^{8,9,14} have been used to study "strong" states up to 3.6 MeV, whereas the (p,d) reaction⁷ has been used to study states up to 4.76 MeV. However, because of ~ 100 keV resolution in the previous (p,d) work, many levels could not be resolved.

Samples of some selected angular distributions are shown in Figs. 2 and 3 for the (p,d) and the (d,t) reactions, respectively. The state at 1.36 MeV is assumed to be a positive-parity state with $J = \frac{7}{2}$ in the Nuclear Data summary.⁵ However, neither the (p,d) nor the (d,t) angular distribution is fitted very well with an $l=4$ transfer. Although Moinester *et al.*⁷ and Diehl *et al.*⁹ assign

TABLE I. Optical-model and FRNL parameters used in DWBA calculations (MeV fm units).

Particle	V	r_0	a	W	$4W_D$	r_I	a_I	r_c	V_{so}	r_{so}	a_{so}	β^2 ^a	R^b
p ^c	48.31	1.17	0.75	5.84	14.6	1.32	0.60	1.30	14.6	1.01	0.75	0.85	
d ^d	100.8	1.099	0.835		53.64	1.344	0.747	1.30	13.06	1.099	0.835	0.54	0.695
t ^e	151.1	1.24	0.685	24.06		1.432	0.870	1.30				0.25	0.845
n		1.15	0.65			$\lambda_{so}=25$						0.85	

^a Nonlocal parameter used in DWUCK.

^b Finite range parameters for (p,d) and (d,t) reactions, respectively, used in DWUCK.

^c Reference 11.

^d Reference 12.

^e Reference 13.

TABLE II. Summary of experimental results for ^{88}Mo .

$^{88}\text{Mo}^*$		C^{25}_n							Nuclear data ^a	
E_x (MeV \pm keV)	l_n	J^π ^b	Present work		Previous work			E_x (MeV)	J^π	
			(p, d)	(d, t)	(d, t) ^c	(d, t) ^d	(p, d) ^e	($^3\text{He}, \alpha$) ^f		
0.0	2	$\frac{5}{2}^+$	1.28	1.24	1.1	1.39	1.25	1.1	0.0	$\frac{5}{2}^+$
0.947 \pm 7	0	$\frac{1}{2}^+$	(0.05)	0.09	0.1	0.20	0.06		0.944	$\frac{1}{2}^+$
1.364 \pm 10	(4)	$\frac{7}{2}^+$	(0.30)	(0.30)		0.08	0.19	0.3	1.364	$(\frac{7}{2})^+$
1.490 \pm 12	$\left\{ \begin{array}{l} 4 \\ +2 \\ +4 \end{array} \right.$	$\frac{9}{2}^+$	0.5		(0.5)	0.67	0.46	0.9	1.4774	$(\frac{9}{2})^+$
		$\frac{3}{2}^+$	0.2		(0.2)	0.24	0.18		1.493	$(\frac{3}{2})^+$
		$\frac{1}{2}^+$				0.06	0.15		1.521	$(\frac{1}{2}, \frac{9}{2})^+$
									1.696	$\frac{5}{2}^+$
								2.146	$(\frac{1}{2})^+$	
								2.182	$(\frac{3}{2})^+$	
								2.249		
2.305 \pm 12	5	$\frac{11}{2}^-$	0.22	0.13			0.24	(0.3)	2.305	$(\frac{11}{2})^-$
									2.362	
2.413 \pm 12	4	$\frac{9}{2}^+$	2.99	2.62	3.5		3.23	3.8	2.409	$(\frac{9}{2})^+$
									2.41	$(\frac{3}{2}, \frac{5}{2})^+$
									2.437	$\frac{1}{2}^+$
									2.443	
									2.484	
									2.529	
2.523 \pm 12	4	$\frac{9}{2}^+$	1.97	1.95			1.79	2.6	2.536	$(\frac{9}{2})^+$
	+1	$\frac{1}{2}^-$	0.39	0.39			0.53		2.56	$(\frac{1}{2}, \frac{3}{2})^-$
									2.576	
2.619 \pm 15	1	$\frac{3}{2}^-$	0.08	0.06					2.645	$(\frac{1}{2}, \frac{3}{2})^-$
									2.673	
2.695 \pm 15	1	$\frac{3}{2}^-$	0.03	0.04			0.08		2.69	$\frac{1}{2}^+$
	+4	$\frac{9}{2}^+$	0.10	0.09			0.11		2.705	$\frac{1}{2}^+$
									2.734	
									2.763	
									2.825	
									2.842	
2.857 \pm 15	1	$\frac{3}{2}^-$	0.08	0.07			0.14		2.872	
									2.881	
									2.904	$(\frac{7}{2}, \frac{9}{2})^+$
2.959 \pm 15	1	$\frac{3}{2}^-$	0.28	0.20			0.41		2.93	$(\frac{1}{2}, \frac{3}{2})^-$
									2.98	
									3.03	$(\frac{7}{2}, \frac{9}{2})^+$
3.064 \pm 15	1	$\frac{3}{2}^-$	0.32	0.24			0.42		3.04	$(\frac{1}{2}, \frac{3}{2})^-$
									3.08	
									3.160	$(\frac{3}{2})^+$

TABLE II (Continued)

$^{95}\text{Mo}^*$			C^{2S}_n						Nuclear data ^a	
E_x (MeV \pm keV)	l_n	J^π ^b	Present work		Previous work			E_x (MeV)	J^π	
			(p, d)	(d, t)	(d, t) ^c	(d, t) ^d	(p, d) ^e	($^3\text{He}, \alpha$) ^f		
3.211 \pm 15	1	$\frac{3}{2}^-$	0.78	0.61	1.0		1.19	(0.5)	3.19	$(\frac{1}{2}, \frac{3}{2})^-$
3.303 \pm 17	4	$\frac{9}{2}^+$	0.24	0.24			0.42	0.5	3.27	$(\frac{7}{2}, \frac{9}{2})^+$
	+1	$\frac{3}{2}^-$	0.19	0.19			0.16			
3.38 \pm 20	2	$\frac{5}{2}^+$	0.08	0.07					(3.441)	
3.434 \pm 17	2	$\frac{5}{2}^+$	0.20	0.22			0.21	0.5	3.450	$(\frac{5}{2})^+$
3.51 \pm 20	4	$\frac{9}{2}^+$	0.30	0.42			0.40		3.57	$(\frac{9}{2})^+$
3.59 \pm 20	1	$\frac{3}{2}^-$	0.14	0.15			0.18	2.0	3.596	$(\frac{3}{2})^+$
	+4	$\frac{9}{2}^+$	1.06	1.10						
3.65 \pm 20	4	$\frac{9}{2}^+$	0.38	0.51			1.49			
3.72 \pm 20	1	$\frac{3}{2}^-$	(0.07)	0.11				(0.10)		
3.79 \pm 20	1	$\frac{3}{2}^-$	0.07	0.06						
3.98 \pm 20	1	$\frac{3}{2}^-$	0.16	0.12			0.25		3.985	
4.07 \pm 20	1	$\frac{3}{2}^-$	0.03							
	+3	$\frac{5}{2}^-$	0.28	0.30						
(4.17)										
4.24 \pm 20	1	$\frac{3}{2}^-$	(0.08)				0.09			
4.37 \pm 20	1	$\frac{3}{2}^-$	(0.11)				0.14		4.378	
4.45 \pm 25	1	$\frac{3}{2}^-$	0.33	0.24			0.72		4.45	$(\frac{1}{2}, \frac{3}{2})^-$
4.52 \pm 25	1	$\frac{3}{2}^-$	0.35	0.27						
4.63 \pm 30	1	$\frac{3}{2}^-$	0.10	0.11			0.15			
	+(3,4)	$\frac{5}{2}^-$	(0.15)				(0.17, 0.06)			
4.71 \pm 30	1	$\frac{3}{2}^-$	0.05	0.07						
	+3	$\frac{5}{2}^-$	0.42	0.32						
									4.756	
4.78 \pm 30	1	$\frac{3}{2}^-$	0.02	0.04						
	+4	$\frac{9}{2}^+$	0.12	0.19						
									4.938	
5.00 \pm 30	1	$\frac{3}{2}^-$	0.09	0.10						
	+3	$\frac{5}{2}^-$	0.14							
5.07 \pm 30	1	$\frac{3}{2}^-$	0.20	0.24						
	+4	$\frac{9}{2}^+$	0.32	0.30						
5.15 \pm 30	1	$\frac{3}{2}^-$	0.05	0.07						

^a Reference 5.^b J values are those which seem plausible on a shell-model basis; no assignments have been made.^c Reference 8.^d Reference 9.^e Reference 7.^f Reference 14

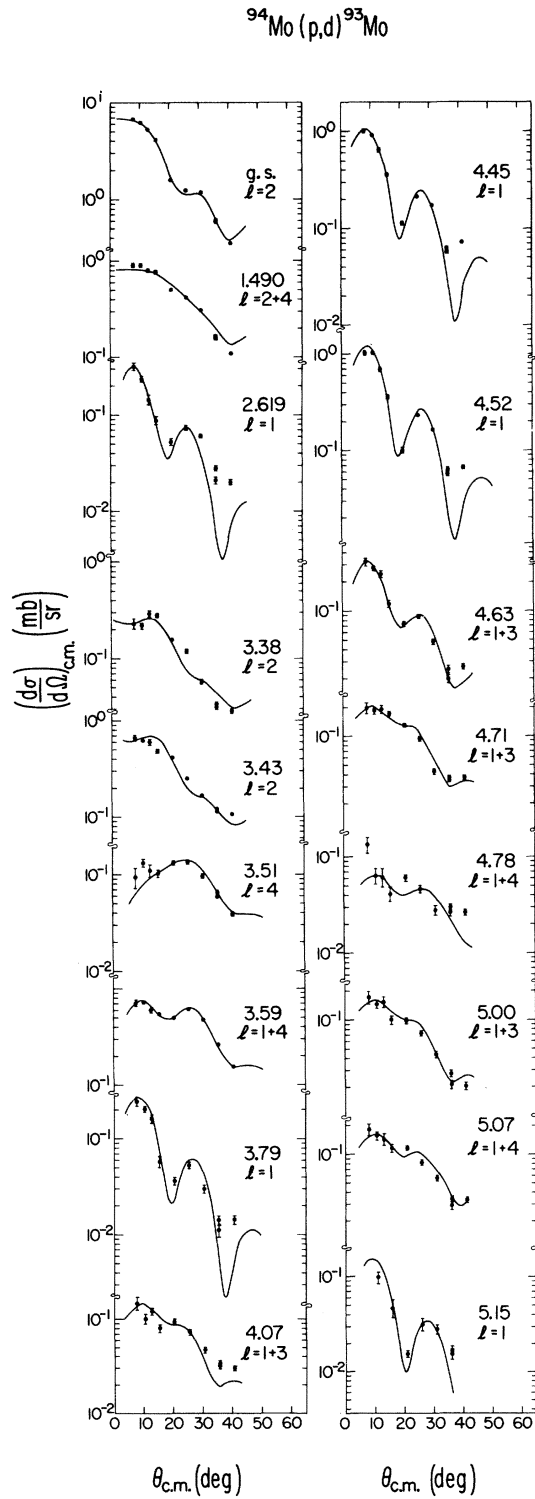


FIG. 2. Angular distributions for the $^{94}\text{Mo}(p,d)^{93}\text{Mo}$ reaction. The errors shown are statistical only. The curves are DWBA calculations for the l transfers indicated.

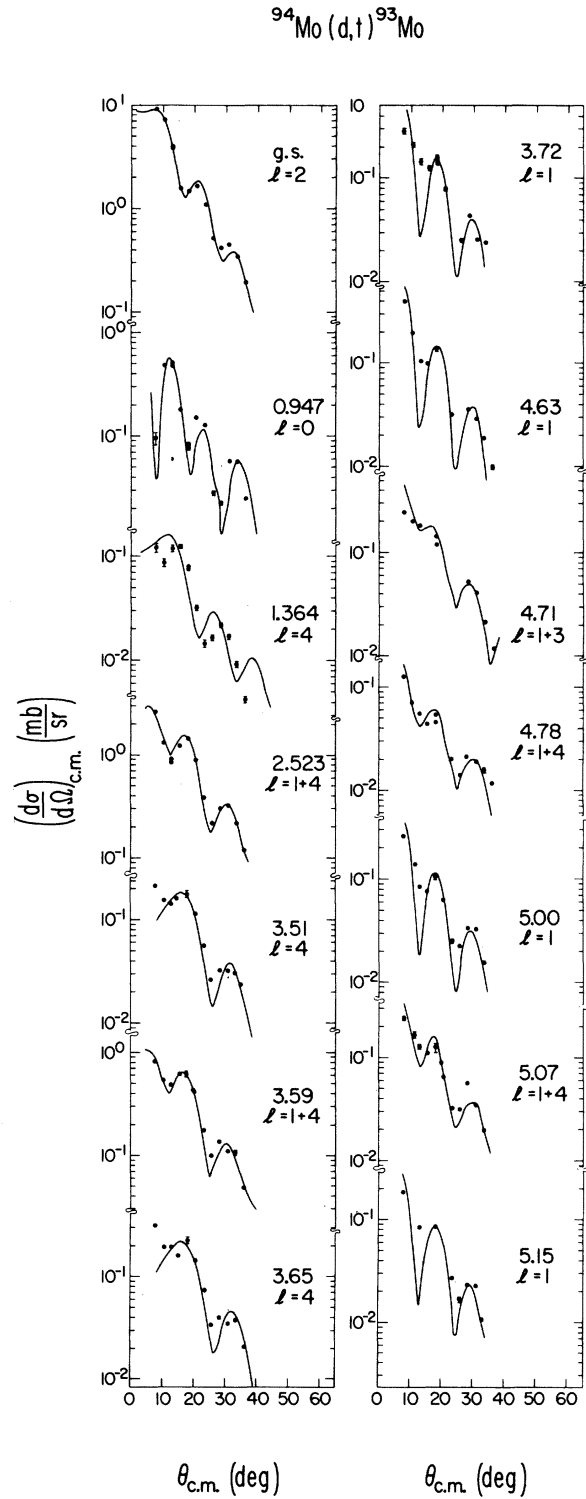


FIG. 3. Angular distributions for the $^{94}\text{Mo}(d,t)^{93}\text{Mo}$ reaction. See Fig. 2 caption.

it $l=4$, their angular distributions are also not fitted well. This is a rather weak state and its excitation could involve higher-order processes.

The two strong $l=4$ states at 2.41 and 2.52 MeV (presumably $\frac{3}{2}^+$) exhaust half of the expected strength for the $1g_{9/2}$ orbital, while a weaker state at 1.477 MeV (possibly $\frac{3}{2}^+$) and a group of states between 3.3 and 5.2 MeV exhaust about 30% of the strength. Although no distinction can be made between $\frac{1}{2}^-$ or $\frac{3}{2}^-$ states in the present experiment, about 60–65% of the total expected wave strength has been observed.

In all we identified 33 groups of states in ^{93}Mo in both the (p,d) and (d,t) reactions. Our analyses show that 22 of the states observed in the (p,d) reaction and 25 in the (d,t) reaction could be fitted by a single l transfer. The main difference in the two studies occurs for highly excited levels, viz., $E \geq 4$ MeV. The angular distributions for the states at 4.07, 4.63, and 5.00 MeV obtained by the (p,d) reaction are fitted by a mixture of two l -transfers, whereas one l value is found to be adequate for the (d,t) reaction. The state at 5.07 MeV could not be fitted in the (p,d) reaction by a mixture of two l transfers; however, the (d,t) data can be fitted reasonably well by $l=1$ and 4. The results of the two analyses for the remaining states in this region are in agreement with each other, as the states at 4.71 and 4.78 MeV required two l transfers and the states at 4.24, 4.37, 4.45, 4.52, and 5.15 MeV were fitted with an $l=1$ transfer in both reactions. The state at 4.17 MeV was observed in both reactions but only at a few angles and no meaningful angular distribution could be obtained for spectroscopic analysis.

B. ^{95}Mo

All the angular distributions obtained along with the DWBA fits for the states analyzed in the $^{96}\text{Mo}(d,t)^{95}\text{Mo}$ reaction are shown in Figs. 4–6. Samples of the fits to the $^{96}\text{Mo}(p,d)^{95}\text{Mo}$ reaction are shown in Fig. 7. The information on energy levels, l -value assignments, and spectroscopic factors for ^{95}Mo obtained in the present study is summarized and compared with previous studies in Table III. Our excitation energies and spectroscopic factors agree well with other studies except for the weakly excited $\frac{1}{2}^+$ states at 0.786 and 1.039 MeV which we did not observe. We have analyzed 28 groups of levels in the $2.6 \leq E_x \leq 4.8$ MeV region observed in the (p,d) and (d,t) data. The energies, l assignments, and spectroscopic factors are in agreement in both reactions. Most of these levels correspond to an $l=1$ transfer, although about 25% of the expected $g_{9/2}$ strength also

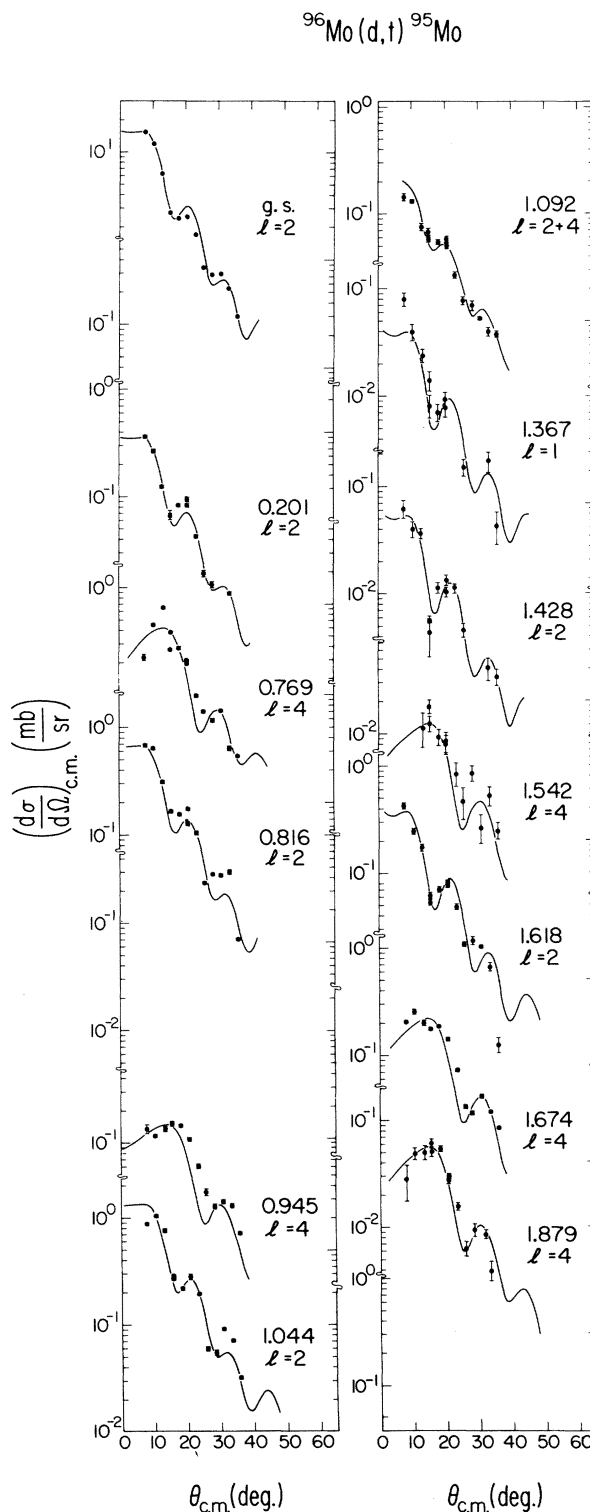


FIG. 4. Angular distributions for the $^{96}\text{Mo}(d,t)^{95}\text{Mo}$ reaction. See Fig. 2 caption.

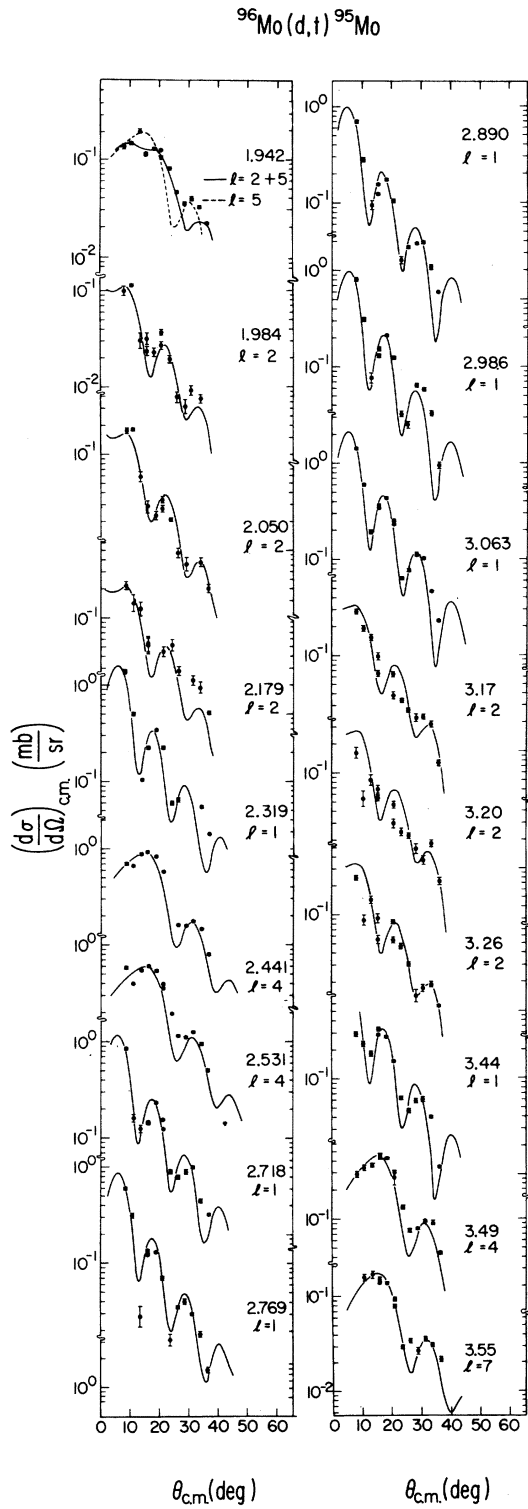


FIG. 5. Angular distributions for the $^{96}\text{Mo}(d,t)^{95}\text{Mo}$ reaction. See Fig. 2 caption.

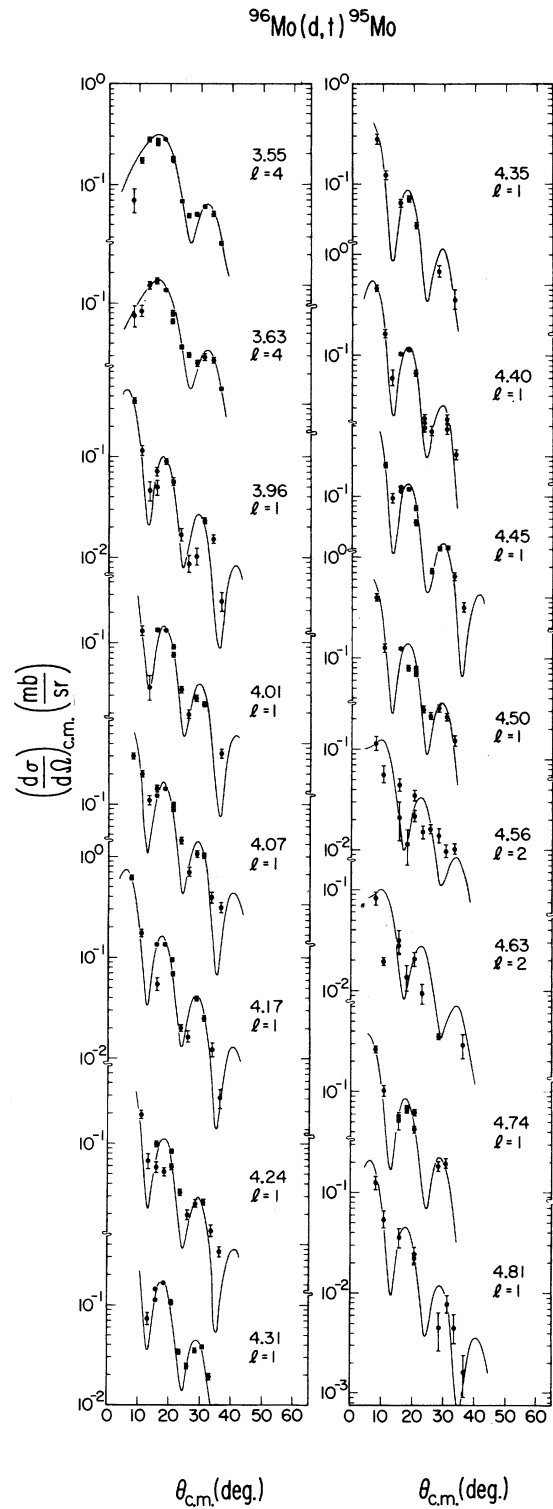


FIG. 6. Angular distributions for the $^{96}\text{Mo}(d,t)^{95}\text{Mo}$ reaction. See Fig. 2 caption.

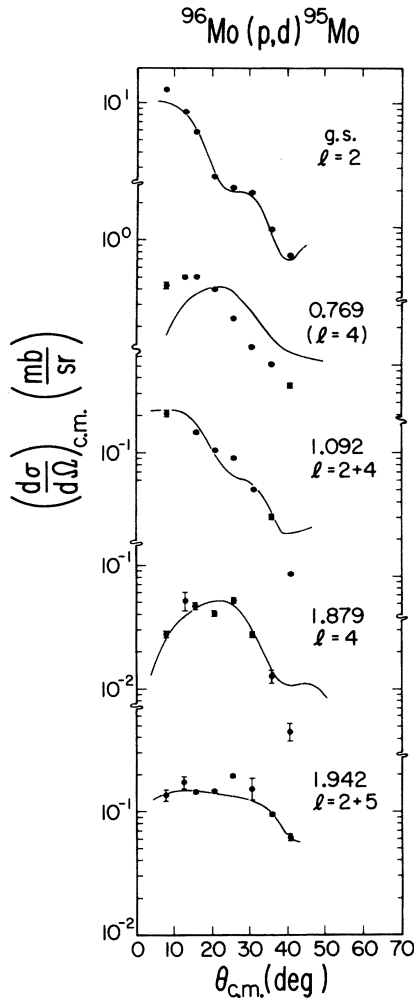


FIG. 7. Angular distributions for the $^{96}\text{Mo}(p,d)^{95}\text{Mo}$ reaction. See Fig. 2 caption.

lies in this energy region. The levels in this region appear to fall into four groups, the first ranging from 2.72 to 3.06 MeV corresponding to $l=1$ transfer, the second from 3.17 to 3.31 MeV with an $l=2$ transfer, the third from 3.38 to 3.63 MeV with an $l=4$ transfer, and the fourth from 3.96 to 4.81 MeV with an $l=1$ transfer.

IV. STRUCTURE CALCULATIONS

Shell-model calculations¹⁶⁻¹⁸ using $2p_{1/2}$, $1g_{9/2}$ proton and $2d_{5/2}$ neutron configurations and core-coupling model calculations,¹⁹ where a two- or three-phonon core is coupled to valence neutrons, have been done with some success for low-lying levels in $^{93,95}\text{Mo}$. Recently we used a quasiparticle-core coupling model to predict the proton hole states of the Nb isotopes² and neutron hole states⁴ of $^{97,99}\text{Mo}$, with reasonable success. We have also

applied this model to the positive-parity $\frac{1}{2}^+$ through $\frac{13}{2}^+$ states in ^{93}Mo and ^{95}Mo by coupling of the neutrons in the $3s_{1/2}$, $2d_{3/2}$, $2d_{5/2}$, $1g_{7/2}$, and $1g_{9/2}$ orbitals with the 0^+ ground state and the first 2^+ excited state of ^{94}Mo and ^{96}Mo , respectively. Quasiparticle energies and occupation numbers are given in Table IV. The values of Hamiltonian parameters χ_1 , χ_2 , and ξ , defined in Ref. 4, are shown in Table V.

A. ^{93}Mo

Theoretical and experimental results for ^{93}Mo are shown in Fig. 8. There are seven known states below 2 MeV in excitation. Six have been observed in pickup reactions while the seventh state at 1.696 MeV has been observed in the (p,t) reaction²⁰ and $(p,n\gamma)$ type reactions (see, for example, Ref. 21). The spins and parities of all these levels are reasonably certain. The present calculations also predict seven levels below 2 MeV which agree in J^π assignments and give reasonable spectroscopic factors for $l=0$ and $l=2$. However, the weak $\frac{5}{2}^+$ state predicted at 1.98 MeV probably corresponds to the known $\frac{5}{2}^+$ state at 1.696 MeV. Furthermore, a weak $\frac{3}{2}^+$ state is predicted at 2.10 MeV which could correspond to the state at 2.182 MeV presumed to be $(\frac{3}{2})^+$. The model predicts a very strong $\frac{9}{2}^+$ level at 2.46 MeV which exhausts about 74% of $1g_{9/2}$ strength but the splitting into two levels observed in the experiment is not reproduced in the calculations. A weak $\frac{1}{2}^+$ level predicted at 2.50 MeV could correspond to the $\frac{1}{2}^+$ level at 2.437 MeV observed in the (d,p) work. At higher energy, the fit is not expected to be good, as one would need to couple several core states to the neutron states to reproduce the large level density for the $l=1$ and 4 states.

B. ^{95}Mo

Experimental and calculated results for ^{95}Mo are shown in Fig. 9. There are nine known positive-parity states below 1.2 MeV in excitation. The calculations predict eight levels below this energy. There is one weak $\frac{1}{2}^+$ state predicted at 0.53 MeV in this energy region, whereas two weak $\frac{1}{2}^+$ states, at 0.79 and 1.04 MeV, are known. Four definite $l=2$ states are known from previous work in this energy region, whereas our analyses of both the (d,t) and (p,d) reactions indicate another $l=2$ level at 1.09 MeV. The theory predicts these levels very nicely except for the lowest $\frac{3}{2}^+$ level at 0.20 MeV. This level is excited very weakly both in the pickup reactions ($C^2S_n \approx 0.05$) and in the stripping reaction ($C^2S_n \approx 0.02$).²³ The known properties of $l=4$ levels in this energy region are predicted very well.

TABLE III. Summary of experimental results for ^{95}Mo .

^{95}Mo E_x (MeV \pm keV)	l_n	J^π ^b	Present work		C^2S_n			Nuclear data ^a		
			(p, d)	(d, t)	(d, t) ^c	Previous work (d, t) ^d	($^3\text{He}, \alpha$) ^e	E_x (MeV)	J^π	
0.0	2	$\frac{5}{2}^+$	1.98	2.54	2.54	1.7	2.58	0.0	$\frac{5}{2}^+$	
0.201 \pm 6	2	$\frac{3}{2}^+$	0.05	0.04	(0.07)	0.1	0.10	0.204	$\frac{3}{2}^+$	
0.769 \pm 6	4	$\frac{7}{2}^+$	(0.88)	0.89	0.81			0.45	0.766	$\frac{7}{2}^+$
					0.15	0.2			0.786	$\frac{1}{2}^+$
0.816 \pm 7	2	$\frac{3}{2}^+$	0.16	0.16	0.21	0.5	0.14	0.821	$(\frac{3}{2}, \frac{5}{2})^+$	
0.945 \pm 7	4	$\frac{9}{2}^+$	0.26	0.18	0.33			0.22	0.948	$\frac{9}{2}^+$
					0.20	0.2			1.039	$\frac{1}{2}^+$
1.044 \pm 10	2	$\frac{5}{2}^+$	0.18	0.18	0.19		0.10	1.059	$(\frac{3}{2}, \frac{5}{2})^+$	
1.092 \pm 12	4	$\frac{7}{2}^+$	0.06	0.05				1.074	$(\frac{7}{2})^+$	
					+2	$\frac{5}{2}^+$	0.04	0.04		
								1.310	$\frac{1}{2}^+$	
1.367 \pm 15	1	$\frac{1}{2}^-$	0.02	0.02				1.376	$(\frac{3}{2}, \frac{5}{2})^+$	
1.428 \pm 12	2	$\frac{3}{2}^+$	0.014	0.014	0.02			1.433	$(\frac{3}{2}, \frac{5}{2})^+$	
1.542 \pm 10	4	$\frac{9}{2}^+$	0.034	0.018				1.533	$(\frac{9}{2})^+$	
1.618 \pm 10	2	$\frac{3}{2}^+$	0.079	0.084	0.13	0.1		1.620	$(\frac{3}{2}, \frac{5}{2})^+$	
1.674 \pm 10	4	$\frac{9}{2}^+$	0.35	0.31	0.46		0.19	1.683	$(\frac{7}{2}, \frac{9}{2})^+$	
								1.707	$(\frac{1}{2})^+$	
1.879 \pm 12	4	$\frac{9}{2}^+$	0.11	0.084						
1.942 \pm 12	5	$\frac{11}{2}^-$	0.33	0.24	0.29		0.39	1.938	$(\frac{1}{2})^-$	
								+2	$\frac{9}{2}^+$	0.033
1.984 \pm 15	2	$\frac{5}{2}^+$	(0.024)	0.023	0.054			1.981	$(\frac{3}{2}, \frac{5}{2})^+$	
2.050 \pm 15	2	$\frac{5}{2}^+$	0.03	0.04	0.09			2.057	$(\frac{3}{2}, \frac{5}{2})^+$	
								2.067	$(\frac{1}{2})^+$	
								2.107	$(\frac{3}{2}, \frac{5}{2})^+$	
2.130 \pm 15	4	$\frac{9}{2}^+$	0.06					2.136	$(\frac{7}{2}, \frac{9}{2})^+$	
2.179 \pm 15	2	$\frac{3}{2}^+$	0.02	0.047	0.042			2.181	$(\frac{3}{2}, \frac{5}{2})^+$	
2.240 \pm 15	1	$\frac{1}{2}^-$	0.03	0.03	0.027			2.221	$(\frac{1}{2}, \frac{3}{2})^-$	
								+2	$\frac{5}{2}^+$	0.04
2.319 \pm 12	1	$\frac{1}{2}^-$	0.33	0.18	0.3	0.5	0.37	2.330	$(\frac{1}{2}, \frac{3}{2})^-$	
2.375 \pm 15	0	$\frac{1}{2}^+$	(0.13)					2.337	$\frac{1}{2}^+$	
								+2	$\frac{5}{2}^+$	(0.05)
								2.396	$(\frac{3}{2}, \frac{5}{2})^+$	
2.441 \pm 12	4	$\frac{9}{2}^+$	1.81	1.37	1.82	2.1	1.30	2.441	$(\frac{7}{2}, \frac{9}{2})^+$	
2.501 \pm 15	(4)	$\frac{9}{2}^+$	(0.18)					2.508		
2.531 \pm 12	4	$\frac{9}{2}^+$	1.18	0.88	1.38	1.3	0.92	2.539	$(\frac{7}{2}, \frac{9}{2})^+$	
2.718 \pm 15	1	$\frac{1}{2}^-$	0.22	0.15						
2.769 \pm 15	1	$\frac{1}{2}^-$	0.13	0.11		0.3		2.78	$(\frac{1}{2}, \frac{3}{2})^-$	

TABLE III (Continued)

^{95}Mo E_x (MeV \pm keV)	l_n	J^π ^b	Present work		C^{2S}_n Previous work			Nuclear data ^a	
			(p, d)	(d, t)	(d, t) ^c	(d, t) ^d	($^3\text{He}, \alpha$) ^e	E_x (MeV)	J^π
2.890 \pm 15	1	$\frac{1}{2}^-$	0.18	0.12					
2.986 \pm 17	1	$\frac{1}{2}^-$	0.17	0.13					
3.063 \pm 17	1	$\frac{1}{2}^-$	0.35	0.29		0.2	3.1		$(\frac{1}{2}, \frac{3}{2})^-$
3.17 \pm 20	2	$\frac{3}{2}^+$	0.06	0.07					
3.20 \pm 20	(2)	$\frac{3}{2}^+$		(0.04)					
3.26 \pm 20	2	$\frac{3}{2}^+$	0.07	0.07					
3.31 \pm 20	2	$\frac{3}{2}^+$	0.04						
3.380 \pm 17	4	$\frac{9}{2}^+$	0.59				0.36		
3.443 \pm 17	1	$\frac{1}{2}^-$	0.20	0.21			0.20	3.48	$(\frac{1}{2}, \frac{3}{2})^-$
3.494 \pm 17	4	$\frac{9}{2}^+$	1.0	0.99			0.81		
3.551 \pm 17	4	$\frac{9}{2}^+$	0.65	0.63			0.25		
3.625 \pm 17	4	$\frac{9}{2}^+$	0.31	0.33					
3.96 \pm 20	1	$\frac{3}{2}^-$	0.084	0.065					
4.01 \pm 20	1	$\frac{3}{2}^-$	0.14	0.12					
4.07 \pm 20	1	$\frac{3}{2}^-$	0.15	0.10					
4.17 \pm 20	1	$\frac{3}{2}^-$	0.13	0.11					
4.24 \pm 20	1	$\frac{3}{2}^-$	0.12	0.12					
4.31 \pm 20	1	$\frac{3}{2}^-$	0.12	0.11					
4.35 \pm 20	1	$\frac{3}{2}^-$	0.14	0.06					
4.40 \pm 25	1	$\frac{3}{2}^-$	0.09	0.08					
4.45 \pm 25	1	$\frac{3}{2}^-$	0.14	0.08					
4.50 \pm 25	1	$\frac{3}{2}^-$	0.13	0.09					
4.56 \pm 30	2	$\frac{3}{2}^+$	0.03	0.04					
4.63 \pm 30	(2)	$\frac{3}{2}^+$	(0.02)	(0.03)					
4.74 \pm 30	1	$\frac{3}{2}^-$	0.08	0.05					
4.81 \pm 30	1	$\frac{3}{2}^-$	0.04	0.03					

^a Reference 6.^b J values are those which seem plausible on a shell-model basis; no assignments have been made.^c Reference 8.^d Reference 9.^e Reference 15.

V. DISCUSSION

According to a simple shell-model picture, the neutron orbits up through the $1g_{9/2}$ orbit are completely filled in ^{92}Mo ($N=50$), and higher orbitals, viz., $2d_{5/2}$, $3s_{1/2}$, $1g_{7/2}$, etc., start getting filled as more neutrons are added. Pickup reactions serve to measure the occupancies of the levels in and below the Fermi surface, whereas stripping reactions provide complementary information about the vacancies of the levels in and above the

Fermi surface. In Table VI, we present the averages of the total strengths of the various orbitals observed for $^{92,94,96,98,100}\text{Mo}$ targets using (p, d) and (d, t) reactions at this laboratory^{1-4, 22} and (d, p) reactions from the literature.²³⁻²⁵ We identify the subshells by their l values, since definite J assignments cannot be made in the one-particle transfer reaction studies. The information on the particle states of ^{101}Mo is very scanty, so little can be said about the unfilled levels of ^{100}Mo .

From Table VI one finds immediately that almost

TABLE IV. Quasiparticle energies and occupancy numbers used in the calculations for ^{93}Mo and ^{95}Mo .

State	^{93}Mo		^{95}Mo	
	Energy (MeV)	V^2	Energy (MeV)	V^2
$3s_{1/2}$	1.6	0.1	2.0	0.15
$2d_{3/2}$	2.1	0.03	2.0	0.15
$2d_{5/2}$	0.0	0.25	0.0	0.35
$1g_{7/2}$	1.5	0.2	1.0	0.16
$1g_{9/2}$	2.4	0.8	2.9	0.97

all the $l=0$ and 2 strength has been accounted for in the Mo isotopes except for ^{98}Mo and ^{100}Mo , where 40% of $l=2$ strength is still unobserved up to 4.5 MeV in excitation. Although some $l=3$ strength is observed in lighter isotopes, no definite level corresponding to $l=3$ has been observed in pickup reactions on $^{96,98,100}\text{Mo}$. This indicates that $1f$ levels are very far away from the Fermi surface and the strength is probably very diluted. With the exception of ^{96}Mo , much of the $l=4$ (possibly $1g_{7/2}$) strength has not been accounted for, and only small amounts have been seen in stripping reactions. The results of pickup reaction studies indicate that much of the $l=4$ hole strength (possibly $1g_{9/2}$) has been observed for light Mo isotopes but less than half is observed for ^{100}Mo .

The hole strength distributions for $l=1$ and 4 are displayed in Fig. 10 for all the Mo isotopes. It is apparent from this figure that the states corresponding to $1g_{9/2}$, $2p_{1/2}$, and $2p_{3/2}$ orbitals, which are the first three discrete states in ^{91}Mo , are split into many levels as neutrons are added. In all Mo isotopes it appears (see also Table VII) that the $l=1$ levels are split into two groups separated by a group of levels corresponding to $l=4$, although level density and the width of each group increases and the strength is diluted in the heavier isotopes. It is expected that most of the lower $l=1$ group corresponds to $2p_{1/2}$ and most of the higher $l=1$ group corresponds to $2p_{3/2}$. If such is the case, most of the strength corresponding to $2p_{1/2}$ has been observed in all the Mo isotopes, whereas much of the $2p_{3/2}$ strength is yet to be seen, particularly in the heavier isotopes. Less than half of the $1g_{9/2}$ strength has been observed in ^{99}Mo ,

TABLE V. Parameters for the hole-core coupling model.

Nucleus	ξ (MeV)	χ_1 (MeV fm $^{-2}$)	χ_2 (MeV fm $^{-2}$)
^{93}Mo	0.05	0.24	-0.08
^{95}Mo	0.0	0.25	-0.10

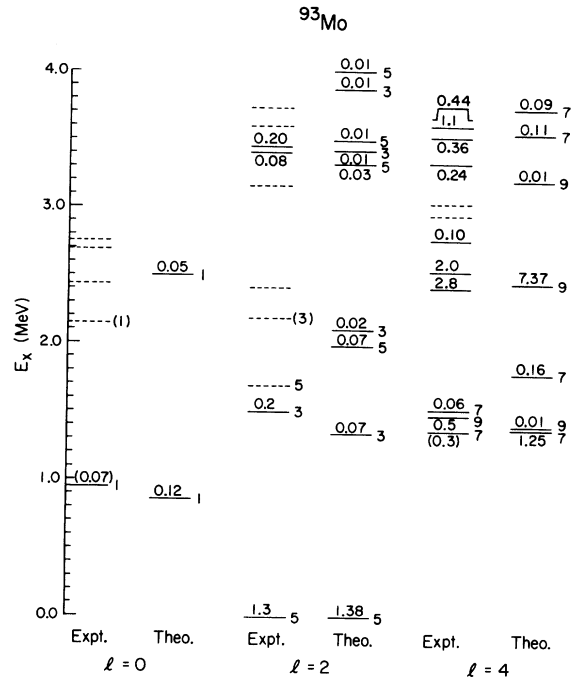


FIG. 8. Comparison of the experimentally observed $l=0, 2,$ and 4 energy levels with the theoretical predictions for ^{93}Mo . The experimental and calculated spectroscopic factors are indicated in the middle of the lines and the theoretical predictions and experimental assignments for $2 \times J$ (wherever known) are indicated on the right of the line. Known levels not observed in this work are indicated by dashed lines.

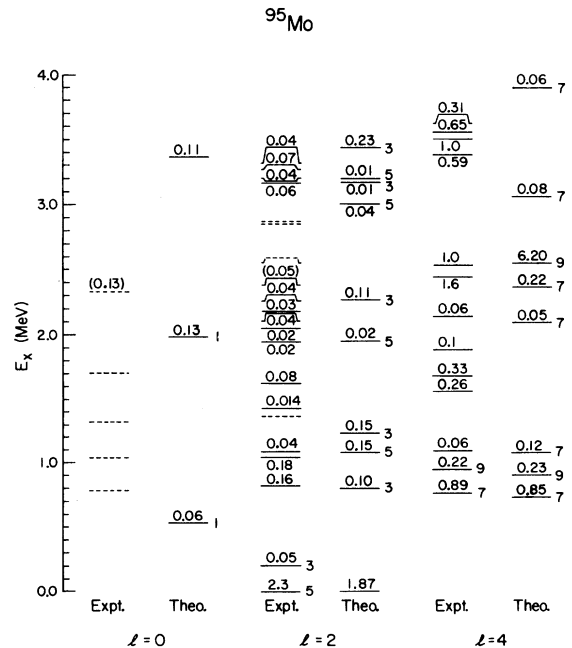


FIG. 9. Comparison of experimentally observed positive-parity states with theoretical predictions for ^{95}Mo . See Fig. 8 caption.

TABLE VI. Summary of neutron stripping [$h=(2J+1)C^2S_n$] and pickup ($p=C^2S_n$) spectroscopic factors for the Mo isotopes. The sum ($T=h+p$) is the total strength accounted for in the l orbital, and the shell-model T value is shown in brackets () at the top of each column.

Target		l						E_x (MeV)	Reference
		2 (10)	0 (2)	4 (18)	5 (12)	1 (6)	3 (6)		
^{92}Mo	p	0.20	0.02	9.15		4.08	3.42	<3.46	22
	h	10.26	2.12	3.60	3.96			<3.23	23
	T	(10.5)	(2.1)	(12.8)					
^{94}Mo	p	1.74	0.07	8.3	0.18	3.72	1.3	<5.15	Present work
	h	8.24	1.6	2.8	3.12			<3.18	23
	T	(10.0)	(1.7)	(11.1)					
^{96}Mo	p	3.23		7.1	0.28	2.6		<4.81	Present work
	h	8.34	1.8	(11.7)	4.75	(0.085)	(0.52)	<4.2	24
	T	(11.6)	(1.8)	(18.8)					
^{98}Mo	p	3.62	0.44	6.18	0.30	2.32		<4.4	4
	h	4.18	1.60	5.12	1.68			<1.9	23
	T	(7.8)	(2.0)	(11.3)					
^{100}Mo	p	3.61	0.22	4.27	0.07	2.29	(0.26)	<4.24	4
	h	2.32	1.22					<0.898	25
	T	(5.9)	(1.4)	(4.27)					

indicating that $1g_{9/2}$ strength is distributed over a large energy range. This could be explained in a particle-hole quadrupole coupling model where the occupied positive-parity states (such as $1g_{9/2}$)

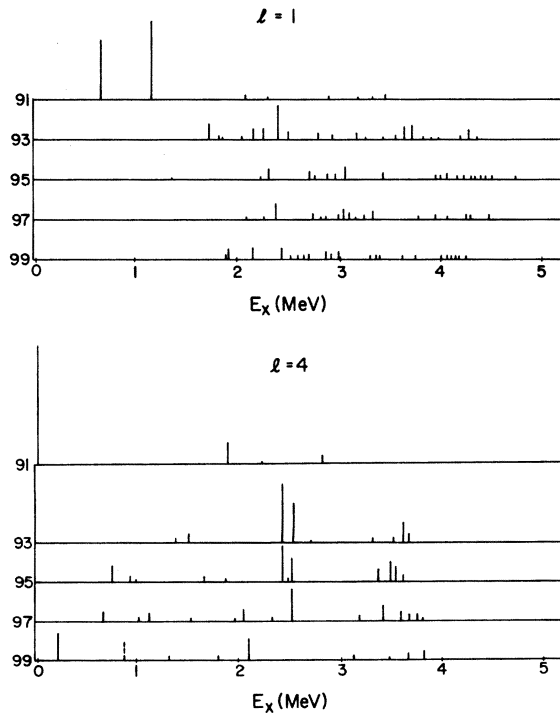


FIG. 10. The hole strength distributions for $l=1$ and 4 for the odd Mo isotopes.

are influenced by the existence of positive-parity valence particles, whereas the negative-parity states (such as $2p_{1/2}$) are not since there are no negative-parity valence particles. This effect will increase the spreading of $1g_{9/2}$ states as the collectivity increases.

Much of the unobserved strength lies presumably in the higher excitation energy region. Analysis²⁶ of the continuum for $E_x \geq 5$ MeV in ^{93}Mo has suggested the presence of considerable $l=1$ strength. For example, the data in the region of excitation energy of 7–8 MeV are consistent with an $l=1$ strength corresponding to $C^2S_n \approx 0.24$. More complete analysis may permit the identification of missing strengths.

VI. CONCLUSIONS

The (p, d) and (d, t) reactions have been used to excite the neutron hole states of ^{93}Mo and ^{95}Mo . A DWBA analysis was used to make assignments and to obtain spectroscopic factors for levels up to 5.15 MeV in ^{93}Mo and 4.81 MeV in ^{95}Mo . The results for the low-lying levels agree with previous studies but many new states have been identified, in particular for ^{95}Mo . Most of the $l=2$ and 4 and part of the $l=1$ strengths have been observed. Some $l=3$ strength has been located in ^{93}Mo but no definite $l=3$ assignment could be made in ^{95}Mo .

A simple core-coupling model using a quasi-particle formalism was used to predict energies, J^π values, and spectroscopic factors for the hole

TABLE VII. Summary of groups of $2p$ and $1g_{9/2}$ hole strength.

A	J^π ^a	E_x ^b (MeV)	C ² S	J^π ^a	E_x (MeV)	C ² S	J^π ^a	E_x (MeV)	C ² S
91	$\frac{1}{2}^-$	0.65(1)	1.58	$\frac{9}{2}^+$	0.0(1)	7.9	$\frac{3}{2}^-$	1.15(1)	1.94
93	$\frac{1}{2}^-$	2.5–3.3(8)	1.93	$\frac{9}{2}^+$	3.3–3.7(4)	2.11	$\frac{3}{2}^-$	3.6–5.2(15)	1.90
95	$\frac{1}{2}^-$	2.3–3.4(7)	1.57	$\frac{9}{2}^+$	3.3–3.7(4)	2.55	$\frac{3}{2}^-$	3.9–4.8(12)	1.19
97	$\frac{1}{2}^-$	2.1–3.4(12)	1.74	$\frac{9}{2}^+$	3.1–3.8(6)	2.27	$\frac{3}{2}^-$	3.8–4.5(7)	0.55
99	$\frac{1}{2}^-$	1.9–3.4(14)	1.75	$\frac{9}{2}^+$	3.1–3.8(5)	0.82	$\frac{3}{2}^-$	3.6–4.3(7)	0.45

^a J value assumed from location (see text).

^b The number of levels in each group is indicated in parentheses beside the energy region.

states in ⁹³Mo and ⁹⁵Mo. Reasonably good agreement was obtained for low-lying states in both nuclei. Analysis of higher excited states would require a more sophisticated model.

Some interesting trends are observed from the systematics of the strength distributions of $l=1$ and 4 in Mo isotopes. It is noted that the almost unfragmented $1g_{9/2}$, $2p_{1/2}$, and $2p_{3/2}$ levels seen

in ⁹¹Mo are split into many levels as neutrons are added. The $2p$ strength is clustered in two separate regions with a group of $l=4$ levels located between them. Most of the $2p_{1/2}$ strength has probably been observed in all the Mo isotopes but part of the strength corresponding to $1g_{9/2}$ and $2p_{3/2}$ is still missing, particularly in the heavier isotopes.

*Supported in part by the National Science Foundation and the Robert A. Welch Foundation.

†Present address: Physics Department, Queen's University, Kingston, Ontario, Canada.

¹D. H. Youngblood and R. L. Kozub, Phys. Rev. Lett. **26**, 572 (1971); Phys. Rev. C **4**, 535 (1971).

²P. K. Bindal, D. H. Youngblood, and R. L. Kozub, Phys. Rev. C **9**, 1618 (1974); *ibid.* **10**, 729 (1974).

³R. L. Kozub and D. H. Youngblood, Phys. Rev. Lett. **28**, 1529 (1972); Phys. Rev. C **7**, 410 (1973).

⁴P. K. Bindal, D. H. Youngblood, R. L. Kozub, and P. H. Hoffmann-Pinther, Phys. Rev. C **12**, 390, 1826 (1975).

⁵D. C. Kocher, Nucl. Data B **8**, 527 (1972).

⁶L. R. Medsker and D. J. Horen, Nucl. Data B **8**, 29 (1972).

⁷M. A. Moinester, G. Finkel, J. Alster, and P. Martin, Nucl. Phys. **202**, 473 (1973).

⁸H. Ohnuma and J. L. Yntema, Phys. Rev. **178**, 1855 (1969).

⁹R. C. Diehl, B. L. Cohen, R. A. Moyer, and L. H. Goldman, Phys. Rev. C **1**, 2132 (1970).

¹⁰Received from P. D. Kunz, University of Colorado (private communication).

¹¹F. D. Becchetti, Jr., and G. W. Greenlees, Phys. Rev. **182**, 1190 (1969).

¹²C. M. Perey and F. G. Perey, Phys. Rev. **152**, 923 (1966).

¹³E. R. Flynn, D. D. Armstrong, J. G. Berry, and A. G. Blair, Phys. Rev. **182**, 1113 (1969).

¹⁴C. M. Fou, Nucl. Phys. **A192**, 139 (1972).

¹⁵J. Schoonover, H. C. Cheung, J. E. Kitching, S. K. Mark, and J. K. P. Lee, Z. Phys. **A272**, 99 (1975).

¹⁶K. H. Bhatt and J. B. Ball, Nucl. Phys. **63**, 286 (1965).

¹⁷N. Auerbach and I. Talmi, Nucl. Phys. **64**, 458 (1965).

¹⁸J. Vervier, Nucl. Phys. **75**, 17 (1966).

¹⁹D. C. Choudhury and J. T. Clemens, Nucl. Phys. **A125**, 140 (1969).

²⁰J. B. Ball, Phys. Lett. **41B**, 55 (1972).

²¹A. Charvet, R. Chery, R. Duffait, and M. Morgue, Nucl. Phys. **A238**, 333 (1975).

²²R. L. Kozub and D. H. Youngblood, Phys. Rev. C **7**, 404 (1973).

²³J. B. Moorehead and R. A. Moyer, Phys. Rev. **184**, 1205 (1969); see also Phys. Rev. C **1**, 2132 (1970).

²⁴L. R. Medsker and J. L. Yntema, Phys. Rev. C **9**, 664 (1974).

²⁵W. L. Sievers, D. A. Close, C. J. Umbarger, R. C. Bearse, and F. W. Prosser, Jr., Phys. Rev. C **6**, 1001 (1972).

²⁶P. K. Bindal and D. H. Youngblood, Bull. Am. Phys. Soc. **21**, 633 (1976).